SQU Journal for Science, 2020, 25(2), 124-129 DOI:10.24200/squjs.vol25iss2pp124-129
Sultan Qaboos University

Magneto-optical Kerr Microscopy for Nano-Structures with Perpendicular Magnetic Anisotropy

Suleiman Al-Risi[1], Rachid Sbiaa[1]*, Hanan Mohammed[2] and Jurgen Kosel[2]

[1]Department of Physics, College of Science, Sultan Qaboos University, P.O. Box 36, Al-Khod, PC 123, Muscat, Oman; [2]King Abdullah University of Science and Technology, Thuwal, 23955-6900, Saudi Arabia. *Email: rachid@squ.edu.om.

ABSTRACT: Magneto-optical Kerr effect (MOKE) microscopy is a powerful imaging technique that can be employed to study the magnetization reversal of thin films and nanoscale structures. In this work, we describe the MOKE microscopy which is used to observe nanomagnetic domain structures of Co/Pt multilayers (MLs) and plot hysteresis loops. We were able to image sub-micrometer size magnetic domains and trace their evolution in a µs time scale with a lateral spatial resolution down to 300 nm. The magnetization reversal for Co/Pt MLs is described by the expansion of the domains in all directions as dendritic domain wall propagation. For a fixed applied magnetic field, the evolution with time of magnetic domains started from many centers, then expanded without the appearance of new nucleated centers. When the applied magnetic field was applied perpendicular to the film plane, a square hysteresis loop was observed indicating that the film exhibits a perpendicular magnetic anisotropy. For the same material, the magnetic field needed to nucleate magnetic domains in sub-micrometer size wire is much larger compared to the thin films. The magnetization decay becomes faster as the applied field is closer to the coercivity of the sample for the thin films MLs. The domain wall (DW) could be manipulated and pinned in a precise location in a stepped nanowire of Co/Pt MLs induced by a consistent magnetic field.

Keywords: Magnetic domain; MOKE microscope; Magnetization reversal; Perpendicular anisotropy; Hysteresis loop.

إستخدام مجهر كيير المغناطيسي الضوئي لدراسة حركة وشكل النطاقات المغناطيسية النانومترية القياس في المواد ذات مغنطة عمودية المغناطيسية

سليمان الريسي، رشيد سبيع، حنان محمد و جورجن كوسل

الملخص: يعتبر مجهر كيير المغناطيسي الضوئي جهاز بكفاءة عالية لدراسة تركيب وحركة النطاقات المغناطيسة بكل القياسات النانومترية أو الميكرومترية لعينات المواد المغناطيسية ، في هذه الدراسة تم صنع وبناء هذا المجهر لدراسة نوع وشكل النطاقات المغناطيسية لمادة $(Co/Ni)_{12}$ ورسم منحنى المغناطيسية لها ، حيث تم تصوير حركة تغير المغناطيسية للمادة بتعريضها لمجال مغناطيسي يتزايد أو ثابت مع الوقت بدقة قياس تصل إلى 300 nm . أوضحت الدراسة أن المغنطة المغناطيسية لهذه المادة تبدأ بتشكل نطاقات نقطيه في أماكن مختلفة ، ثم تنمو بشكل عشوائي باستمرار تعرضها للمجال المغناطيسي، وتأخذ في نموها شكل مشابه لنمو جذور الشجرة حيث تكون متشابكه وتنتشر في كل الاتجاهات. منحنى المغنطه المغناطيسية أوضح أن المادة تمتلك اتجاه مغناطيسي عمودي على اتجاه سطح المادة. هذه الدراسه كشفت أن السلك الميكرومتري يحتاج لمجال مغناطيسي أكبر لظهور النطاق المغناطيسي عن العينه ذات السطح الأكبر مساحه لنفس الماده، وأيضا كلما كان المجال المغناطيسي المعرض للماده قريبا من قيمة الكوريسفيتي للماده كان تغير المغنطه المغناطيسية سريعا، وأخيرا تم دراسة حركة جدارالنطاق المغناطيسي للسلك النانومتري للمادة، وتم التحكم في توقيفه أو حركته باستخدام عدة درجات عمودية على السلك وتعريضه لمجال مغناطيسي والذي يمكن استخدامه مستقبلا في شرائح الذاكرة.

الكلمات المفتاحية: مجهر كيير، النطاقات المغناطيسية، منحنى المغناطيسية، المغناطيسية العمودية.

1. Introduction

Imaging and modeling magnetic micro- and nanostructures are highly desirable due to the large number of applications in many areas. Most of the techniques used for analyzing lateral magnetic nanostructures are powerful and highly advanced, and may have special requirements for sample conditions and thus have limitations. The tools available for imaging magnetic domains are Lorentz microscopy, magnetic force microscopy (MFM), X-ray photoelectron emission microscopy (PEEM), magnetic transmission X-ray microscopy (MTXM) and Kerr microscopy to quote only few of them. On the other hand, for sample characterization and signal detection/measurements, a superconducting quantum interference device (SQUID), the Hall effect, the Bragg-magneto-optic Kerr effect, and polarized neutron reflectivity (PNR) are commonly used [1-2]. Some of these have limitations and are not compatible with the study of magnetic response or reversal of magnetization. For instance, the magnetic force microscopy (MFM) is a high spatial resolution technique to image magnetic nanostructures. However, its main drawbacks are the slow scan speed, the existence of undesirable tip-sample interaction and limitation to the strength of the applied magnetic field as the magnetic tip could be affected by the same applied field. Magneto-optical Kerr effect (MOKE) microscopy is an efficient technique to get detailed and direct insight into the magnetic switching mechanism, as it combines fast measurements, flexibility, high-sensitivity and non-destruction of the sample [1], [3-5]. An additional advantage of this technique is mapping the evolution of the magnetization configuration at any magnetic field or electric current. Hence the idea of building and developing it locally has attracted considerable interest [6]. Its resolution could be enhanced using a short wavelength, oil immersion objective lens and high-resolution camera.

Magnetic materials based on Co/Pt multilayers (MLs) with perpendicular magnetic anisotropy (PMA) are promising candidates for ultrahigh density perpendicular recording [7-15] and magnetic random access memory [14-16] due to their thermal stability in nano-scale devices. It is also easy to adjust these materials intrinsic properties. The coercivity H_c, magnetic anisotropy K_u, and domain size could be tuned either by varying the bilayer repetitions number N or the thicknesses of the sublayers. Submicron sized magnetic domains in thin films and nanowires may play an important role in advanced magnetic storage schemes and thus, their dynamic magnetic properties are being studied experimentally and theoretically. For instance, the magnetic anisotropy, exchange stiffness and the saturation magnetization have an essential effect in defining the nature and stability of domain structure. For magnetic memory applications, as high storage densities are required, it is essential to have the capability to study small magnetic domains and have an insight into their dynamical behavior.

In the present article, a high-resolution MOKE microscope devoted to studying the magnetization reversal induced by a magnetic field and magnetic properties for Co/Pt MLs thin films is described. The unique performances of our set up will be illustrated and demonstrated by studying the domain motion of Co/Pt thin film and nanowire. Then, and for the same material, we show the possibility of moving and pinning DW by a magnetic field for a stepped wire, which could open an avenue for high magnetic memory.

2. Experimental

The samples were deposited by direct current (DC)-sputtering in a high vacuum chamber on a thermally oxidized silicon (SiO2) substrate. The multilayers consisted of [Co (0.3 nm)/Pt(0.8 nm)]. The seed layer was made of Ta (5 nm) and Pt (3nm) and the capping layer made of 3 nm Pt followed by 5 nm Ta to prevent oxidation. Twelve bilayers (Co/Pt) were included. The magnetic measurements were carried out using the magneto-optic Kerr effect microscope at room temperature and indicated that the sample had an easy perpendicular axis. The micro-sized wires were fabricated by electron-beam lithography (EBL) and direct-write laser (DWL) lithography with a width of 1 µm. The wire was patterned to be a stepped device with six nano-constrictions created by an off-set in *x* and *y* directions as described previously [15]. The wires were connected to a nucleation pad at one end (Figure 4 (a-b)). Figure 1 displays a schematic diagram of the MOKE microscope set up. The uniform red light is emitted by a high-intensity light-emitting diode LED (670 nm, 700 mW). The output from the LED is collimated and passes through an aperture to modulate the size of the light spot. The light is then linearly polarized by a polarizer and passes through a beam splitter to be focused on the objective lens by using a convex lens (f =12 cm). The light interacts and is reflected by the metallic surface to be captured again by the objective lens and then passes through the beam splitter. The beam splitter directs the light through an analyzer to be collected towards a charge-coupled-device (CCD) camera (if the imaging function is required) by a convex lens. The sample is placed on a holder attached to a high precision mounting stage that enables shifting the sample with a precision of 0.1 µm. A red laser could replace the LED if hysteresis loop plotting is required and the light passes in the same path as described above. In the latter case, an optical chopper and a photodiode instead of the CCD camera are used. In the present polar geometry, the set-up is equipped with an electromagnet under the sample, which is controlled by a bipolar power supply and provides a magnetic field of up to 300 mT with typical increment steps of 0.001 mT. The CCD camera, the lock-amplifier and the power supply are controlled by computer. This configuration allows us to induce the magnetic field whether in-plane or in a perpendicular direction to the sample surface. Mechanical stability and elimination of vibration are accomplished by using a vibration-free optical table. The polarizer and analyzer are aligned almost perpendicular to each other.

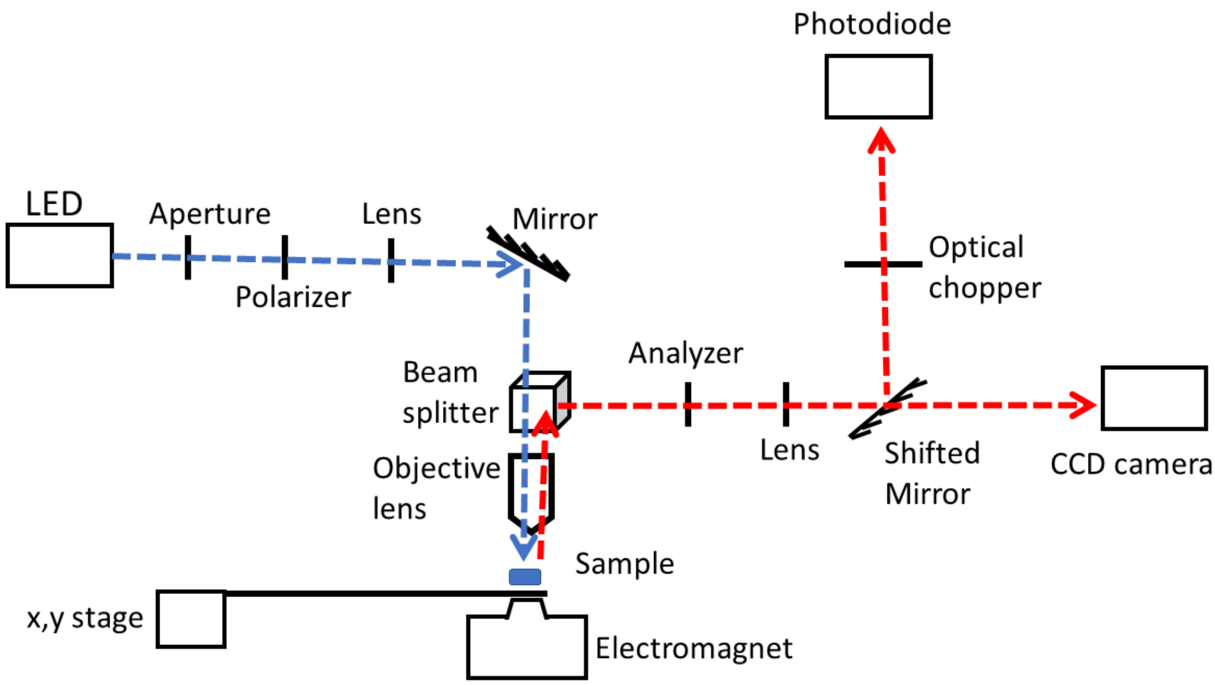

Figure 1. A schematic drawing of the MOKE microscope set up.

This configuration yields to a very weak light intensity, hence the 12-bit and highly sensitive charge coupled device (CCD) camera was used. The direct domain observation was possible for thin film materials without applying any image process technique.

3. Results and discussion

Magnetization reversal versus external magnetic field (M-H) curves of Co/Pt were measured and magnetic domains were imaged by MOKE microscopy at room temperature. Figure 2 shows the M-H curves for the film under in-plane and out-of-plane magnetic fields. When the applied field is in the out-of-plane direction, a clear square hysteresis loop can be observed. On the other an almost S-like shape of the magnetization versus the applied field is revealed for the in-plane applied field case. These two curves indicate that the material exhibits a perpendicular magnetic anisotropy. The magnetization reversal takes place by domain nucleation at a few sites, and is followed by a fast domain wall motion, as shown in Figure 2(a) from the hysteresis loop and inset Kerr images. From the out-of-plane M-H curve, the value of the coercive field and the saturation magnetization extracted from magnetometry measurements are H_c = 41 mT and M_s = 491 emu/cm^3, respectively. The perpendicular anisotropy K_u = 2.73×10^6 erg/cm^3 for the film was calculated from M-H loops out-of-plane and in-plane using Eq. (1).

$$K_u = \int_0^{M_s} \mu_{o\, H_{in}}\, dM - \int_0^{M_s} \mu_{o\, H_{out}}\, dM \qquad (1)$$

where H_{in} and H_{out} are the in-plane and the out-of-plane magnetic fields, respectively, and μ_o is the permeability constant in a vacuum. The domains' evolution under an applied magnetic field perpendicular-to-plane with different strengths and their time dependence under a constant magnetic field was performed at room temperature by MOKE microscopy using high magnification lenses and the images were recorded by a high-resolution camera with a speed of 65 frames/s. The sample was first fully saturated by a large perpendicular-to-plane magnetic field, then retained at the remanence state (no applied magnetic field) and followed by a reverse magnetic field. The selection of domain images is presented in Figure 2(c) and Figure 3(a), in which the bright and dark regions correspond to up and down magnetization states, respectively. It can be seen from Figure 2(c) and Figure 3(a) that the magnetization distribution is dominated by domain wall propagation as a dendritic structure starting from one small nucleation center, of less than one micrometer. Both reversals, due to an incremented applied magnetic field or being time-dependent, look similar, i.e., the domain structures are irregular and the extension of the magnetic domain is along a preferred direction. Moreover, the nucleation was observed in one center only when the lens magnification is more than 40x, which suggests that there are relatively few nucleation centers as described above.

From one saturation state to the opposite saturation state, the reversed area was calculated (difference of contrasts). The magnetization decay from -M_s to +Ms was then measured as a function of time. This was repeated for several values of the applied magnetic field, giving relaxation times less than 300 s. As expected, by increasing the strength of the applied magnetic field, the magnetization reversal is much faster, but no new nucleation centers were observed Figure 3(b). The change in the magnetization due to the rapid domain wall motion is linked to the quality of interfaces between Co and Pt sub-layers and the partial spin-polarization of non-magnetic Pt. This behavior is similar to that observed previously in the Pt(3.4 nm)/Co(1.5 nm)/Pt(6.5 nm) [10].

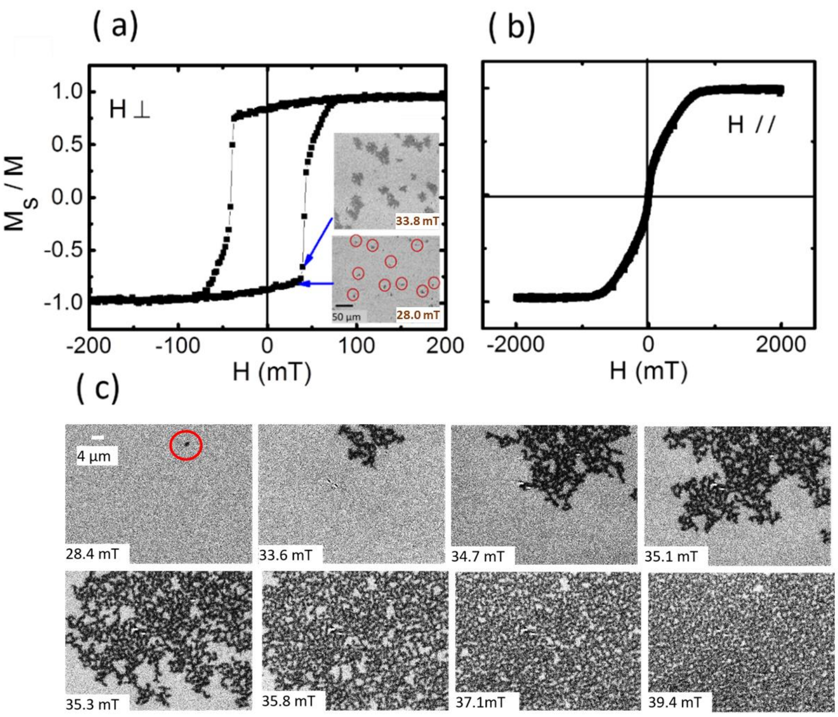

Figure 2. (a) Hysteresis loops of $(Co/Pt)_{12}$ MLs in the out-of-plane direction. The 300 µm × 300 µm using × 4 objective lens MOKE images (insert) of the magnetic domains' nucleation were taken in the beginning of the evolution (b) Hysteresis loops of $(Co/Pt)_{12}$ MLs in the plane to the surface of the film. (c) MOKE images of magnetic domains' evolution with the magnetic field using × 40 objective lens; the field was increased in steps of 0.01 mT/s.

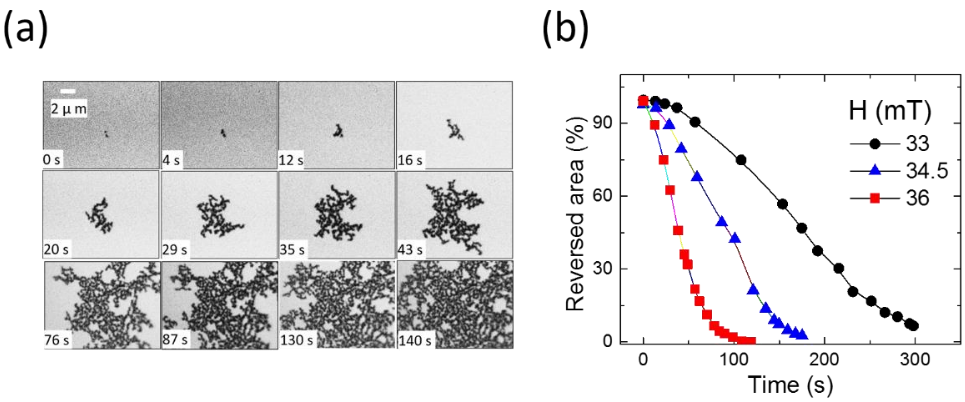

Figure 3. Time-dependent magnetization (a) MOKE images of 10 µm × 11 µm captured after applying a magnetic field of 33 mT. (b) Reversed area of the magnetic domains versus time curves plotted after the application of various reverse magnetic fields.

In the second part of the study, we used the home-built MOKE microscope to image DW position in a stepped wire. The wire was made of the same material as discussed in the first part of this study Figure 4. The constricted (stepped) area is very effective in pinning DW in precise positions as reported theoretically [14] and experimentally for both in-plane and perpendicular anisotropic materials [15-16]. The wire, made of $(Co/Pt)_{\times 12}$, was patterned in 50 µm length and 1 µm width. Along the wire, six nano-constrictions with off-set in *x* and *y* directions, represented by λ and *d*, were created, as can be seen in Figure 4(b), (c). The DW motion could not be observed in the wire under the application of a magnetic field until the wire was annealed at 300 °C for 30 minutes. The annealing process reduces the magnetic anisotropic energy for the wire which leads to a low magnetic field, as required to move the domain wall. The wire was first saturated at 100 mT in the direction perpendicular to the wire plane then a reversal field in continuous steps of 1 mT was applied in the opposite direction. As described in Figure 4(d), it was possible to stabilize the DW at each step by a magnetic field in the stepped wire with d = 600 nm and λ = 0 nm. The positions of DW in the wire were captured using the MOKE microscopy described in Figure 1 and the images presented in Figure 4(c) were obtained by subtracting the actual image from a saturated one (no magnetic domain). To study the movement of DW in the wire by the magnetic field, we started by first applying -60 mT in the out-of-plane direction, which corresponds to the nucleation of magnetic domains in the pad. It is important to note that the nucleation magnetic field for the thin film was 28.4 mT Figure 2(c), which is much smaller than within the pad in the wire. The DW could be moved to the first step by applying -65 mT. The strong pinning field of DW in the first step requires an applied field of -76 mT to de-pin it toward the second step. Consequently, the positioning of DW to the third, the fourth and the fifth steps was achieved by applying magnetic fields of -84, -88 and -90 mT, respectively. Finally, an applied field of -96 mT was needed to align all the domains in one direction (saturation). Again, it was more than double that required for saturation in the case of the thin film. This way of controlling DW in the nano-wire could be used for multiple-bit-per-cell memory, as shown in Figure 4(c). In this example, the device shows eight different states based on nano-constrictions.

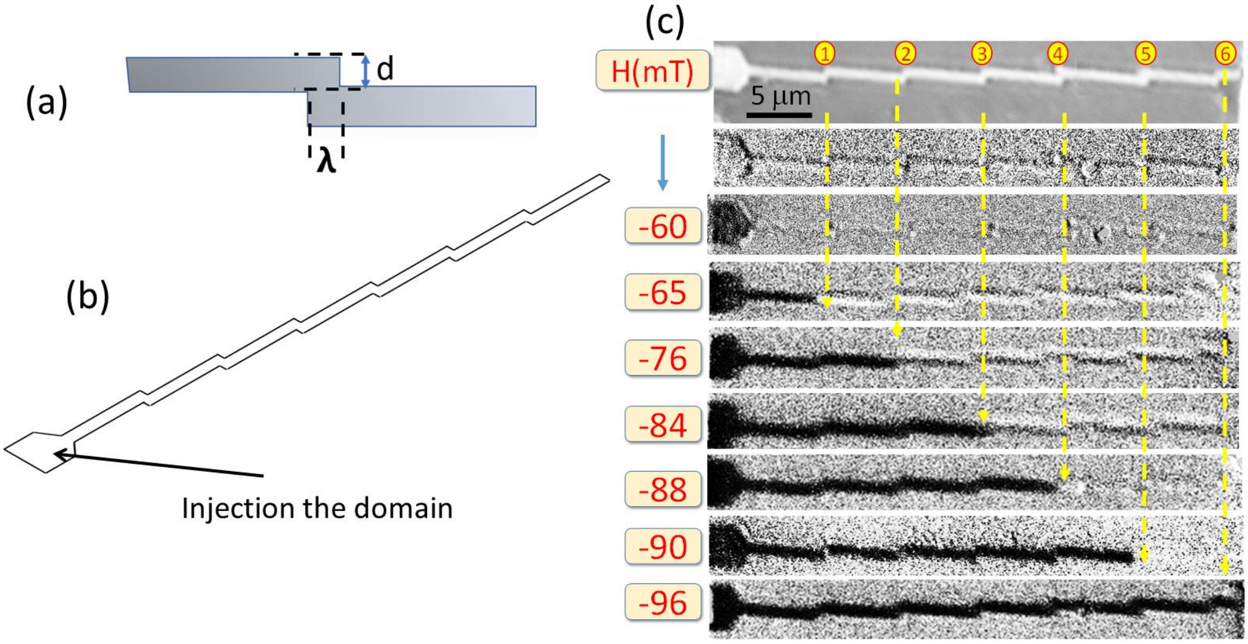

Figure 4. (a) Illustration of the staggered region with the x and y off-sets represented by $\lambda = 0$ and d = 600 nm, respectively. (b) The design of a staggered micro-wire with multi-steps is proposed to control the position of DW. The length and width of wire were fixed at 50 µm and 1 µm, respectively. (c) MOKE images of a fabricated device with six pinning regions. The polar MOKE images of different magnetic states at different applied perpendicular magnetic fields. The device was first saturated using a perpendicular magnetic field of 100 mT, then a reversed field was applied in the opposite direction to move the DW from one step to another.

4. Conclusion

We have demonstrated the magneto-optical Kerr effect method for visualization of magnetic domain dynamics in thin films and nanowire of (Co/Pt) multilayers with 12 repeats. This method was used to image and plot the magnetization reversal process with polar geometry. This study shows that, as the sample size is reduced, there is a need for a higher magnetic field to nucleate magnetic domains and saturate the magnetization of the sample. From MOKE images, the magnetization reversal in $(Co/Pt)_{\times 12}$ multilayers is initiated by small domains randomly distributed in all directions and evolves with time or magnetic field. We have studied the domain-wall motion using MOKE microscopy for a stepped nanowire. It is possible to move and block the domain-wall at a precise position within the $(Co/Pt)_{\times 12}$ nanowire for a certain period of time.

Conflict of interest

The authors declare no conflict of interest.

Acknowledgment

The authors thank Sultan Qaboos University for the financial support under Grant number IG/SCI/PHYS/18/04. The authors would like to thank S. Al Harthi and M.T. Zar Myint from Sultan Qaboos University for their support and assistance in the magnetometry measurements.

References

1. Westphalen, A., Lee, M.S., Remhof, A., and Zabel, H., *Review of Scientific Instruments*, 2007, **78**, 121301.
2. Fischer, P., and Young, M., *IEEE Photonics Journal*, 2010, **2**, 260.
3. Cormier, M., Fert, J., Mougin, A., Cromìres, J.P., and Klein., V., *Review of Scientific Instruments*, 2008, **79**, 033706.
4. Nikulina, E., Idigoras, O., Vavassori, P., Chuvilin, A., and Berger, A., *Applied Physics Letters*, 2012, **100**, 142401.
5. Nistor, C., Beach, G.S.D., and Erskine., J.L., *Review of Scientific Instruments*, 2006, **77**, 103901.
6. Stupakiewicz, A., Chizhik, A., Tekielak, M., Zhukov, A., Gonzalez, J., and Maziewski., A., *Review of Scientific Instruments*, 2014, **85**, 103702.
7. Meng, Z., Kumar, M., Qiu, J., Han, G., Teo, K.L., and Ngo., D.T., *Journal of Physics D: Applied Physics*, 2014, **47**, 43.
8. Ho, P., Zhang, J., Bono, D.C., Chen, J., and Ross., C.A., *IEEE Transactions on Magnetics*, 2016, **52**, 2526972.
9. Parlak, U., Adam, R. D., Bürgler, E., Gang, S., and Schneider., C.M., *Physical Review B*, 2018, **98**, 214443.
10. Kisielewski, M., Maziewski, A., Tekielak, M., Ferré, J., Lemerle, S., Mathet, V., and Chappert, C., *Journal of Magnetism and Magnetic Materials*, 2003, **260**, 231-243.
11. Kumar, D., Jin, T., Al Risi, S., Sbiaa, R., Lew, W.S., and Piramanayagam, S.N., *IEEE Transactions on Magnetics*, 2019, **55**, 2300708.
12. Al Bahri, M., Borie, B., Jin, T.L., Sbiaa, R., Kläui, M., and Piramanayagam., S.N., *Physical Review Applied*, 2019, **11**, 024023.
14. Al Bahri, M., and Sbiaa., R., *Scientific Reports*, 2016, **6**, 28590.
15. Sbiaa, R., and Al Bahri., M., *Journal of Magnetism and Magnetic Materials*, 2016, **411**, 113-115.
16. Mohammed, H., Al Risi, S., Jin, T.L., Kosel, J., Piramanayagam, S.N., and Sbiaa., R., *Applied Physics Letters*, 2020, **116**, 032402.

Received 2 March 2020
Accepted 27 July 2020